

1

2 MR. HERNAN EDUARDO MORALES (Orcid ID : 0000-0002-2964-020X)

3 DR. ALEXANDRA PAVLOVA (Orcid ID : 0000-0001-9455-4124)

4

5

6 Received Date : 16-Oct-2016

7 Revised Date : 14-Mar-2017

8 Accepted Date : 15-Mar-2017

9 Article type : Original Article

10

11

12 Running head: mitochondrial vs. nuclear introgression

13 **Title: Perpendicular axes of differentiation generated by mitochondrial**
14 **introgression**

15 Authors: Hernán E. Morales^{12*}, Paul Sunnucks¹, Leo Joseph³ and Alexandra
16 Pavlova¹

17 1 School of Biological Sciences Monash University, Clayton Campus, Melbourne,
18 3800 Victoria, Australia

19 2 Department of Marine Sciences, University of Gothenburg, Box 461, SE 405 30
20 Göteborg, Sweden

21 3 Australian National Wildlife Collection, CSIRO National Research Collections
22 Australia, GPO Box 1700, Canberra ACT 2601

23 *Corresponding author: hern.moral@gmail.com

24 Date: October 15 2016

25 Word count (main text): 6,472

This is the author manuscript accepted for publication and has undergone full peer review but has not been through the copyediting, typesetting, pagination and proofreading process, which may lead to differences between this version and the [Version of Record](https://doi.org/10.1111/mec.14114). Please cite this article as [doi: 10.1111/mec.14114](https://doi.org/10.1111/mec.14114)

This article is protected by copyright. All rights reserved

26 KEY WORDS: mitochondria, mitonuclear, coalescence, adaptive introgression,
27 selective sweep.

28 **ABSTRACT**

29 Differential introgression of mitochondrial versus nuclear DNA generates discordant
30 patterns of geographic variation and can promote population divergence and
31 speciation. We examined a potential case of mitochondrial introgression leading to
32 two perpendicular axes of differentiation. The Eastern Yellow Robin *Eopsaltria*
33 *australis*, a widespread Australian bird, shows a deep mitochondrial split that is
34 perpendicular to north-south nuclear DNA and plumage colour differentiation. We
35 propose a scenario to explain this pattern: (1) the two nuclear and mitochondrial
36 genomes differentiated in concert during north-south population divergence; (2) later,
37 their histories disconnected after two mitochondrial introgression events resulting in a
38 deep mitochondrial split perpendicular to the nuclear DNA structure. We explored
39 this scenario by coalescent modelling of ten mitochondrial genes and 400 nuclear
40 DNA loci. Initial mitochondrial and nuclear genome divergences were estimated to
41 have occurred in the early Pleistocene, consistent with the proposed scenario.
42 Subsequent climatic transitions may have driven later mitochondrial introgression.
43 We consider neutral introgression unlikely and instead propose that the evidence is
44 more consistent with adaptive mitochondrial introgression and selection against
45 incompatible mitochondrial-nuclear combinations. This likely generated an axis of
46 coastal-inland mitochondrial differentiation in the face of nuclear gene flow,
47 perpendicular to the initial north-south axis of differentiation (reflected in genome-
48 wide nuclear DNA and colour variation).

49 **INTRODUCTION**

50 When divergent populations undergo hybridization, genes from one population can
51 be incorporated into the other (i.e., there is introgression) to a variable extent within
52 and between genomes (Harrison & Larson 2014; Harrison & Larson 2016). Alleles
53 that are not involved in local adaptation and that have not accumulated
54 incompatibilities with other loci are expected to move freely between populations
55 (Mallet 2005). On the other hand, if genes from one population improve fitness in the
56 other population, adaptive introgression can occur (Hedrick 2013). The proportion of
57 the genome that is resistant or prone to introgression can vary as a result of local
58 adaptation in heterogeneous environments and demographic history (Harrison &
59 Larson 2014). Therefore, differential rates of introgression offer a valuable insight
60 into adaptive divergence and speciation (Payseur 2010; Rheindt & Edwards 2011).

61 Differential rates of introgression of mitochondrial DNA (mtDNA) versus
62 nuclear DNA (nDNA) genes are a main cause of mitochondrial-nuclear (mitonuclear)
63 discordances (Toews & Brelsford 2012). However, it is challenging to predict the
64 conditions under which higher rates of mitochondrial or nuclear introgression can be
65 expected. This is because genetic patterns in both genomes can differently reflect
66 the effects of genetic drift and selection, and the two genomes have different modes
67 of inheritance and recombination (Funk & Omland 2003; Harrison 1990). In addition,
68 demographic and ecological factors including population density, sex-ratio, mating
69 behaviour, sex-bias in dispersal and episodes of spatial invasion impact expectations
70 for nuclear and mitochondrial gene flow (Currat *et al.* 2008; Petit & Excoffier 2009).
71 These considerations have generated the counter-intuitive proposal that hybridizing
72 populations will typically experience less gene flow between them in markers that
73 experience more gene flow within populations (Petit & Excoffier 2009). A test of this
74 in 37 case studies revealed that 16/16 hybridization scenarios with female-biased
75 dispersal had less mtDNA than nDNA gene flow between them, while the reverse
76 was true for most male-biased dispersers (Petit & Excoffier 2009). Moreover, low
77 passage through hybrid zones of maternally-transmitted mtDNA is predicted for
78 species with heterogametic females, such as birds, under Haldane's Rule (i.e.
79 disproportional hybrid sterility and/or inviability of the heterogametic sex; Haldane
80 1922). These predictions are commonly supported by studies of avian hybrid zones
81 (Rheindt & Edwards 2011). On the other hand, higher mtDNA than nDNA
82 introgression can occur if a population of low effective size accumulate slightly
83 deleterious mutations by drift (i.e. build up mitochondrial mutation load) to the point
84 where mitochondrial replacement (by introgression) from neighbouring populations is
85 needed (Sloan *et al.* 2016). Moreover, high mtDNA introgression can stem from
86 female-biased dispersal (Petit *et al.* 2004) and asymmetrical mating success of
87 females from hybridizing populations (Roca *et al.* 2005), where females that are
88 more dispersive and/or reproductively successful will transmit maternally inherited
89 mtDNA more often. Alternatively to all the non-adaptive explanations above, adaptive
90 mitochondrial introgression into a beneficiary population could be common given the
91 importance of mtDNA for organismal metabolism and fitness (Currat *et al.* 2008;
92 Hedrick 2013; Toews & Brelsford 2012).

93 The Eastern Yellow Robin (*Eopsaltria australis*, hereafter EYR) shows a
94 striking pattern of geographic mitonuclear discordance, representing an excellent
95 system to study differential mtDNA and nDNA introgression (Pavlova *et al.* 2013).
96 The two major mitochondrial lineages of EYR (mitolineages; mito-A and mito-B) are
97 6.8% divergent and structured across inland and coastal sides of the Great Dividing

98 Range in south-eastern Australia (Pavlova *et al.* 2013; Fig. 1A). In contrast, the major
99 axis of nDNA structure runs north-south through the species range (Fig. 1B). Thus,
100 nDNA and mtDNA structures are geographically perpendicular (Pavlova *et al.* 2013;
101 Fig. 1A-B). Additionally, minor inland-coastal nDNA structure exists in the south
102 corresponding with mitolineage distributions (Morales *et al.* 2016a; Fig. 1B). The
103 major north-south axis of nDNA differentiation is mirrored by rump plumage colour
104 variation, supporting two currently recognized subspecies: the rump is bright yellow
105 in northern *E. a. chrysorrhoa*, and olive-green in southern *E. a. australis* (Ford 1979;
106 Schodde & Mason 1999). Colour variation at the continental-scale is strongly
107 influenced by population history, but on a regional scale appears to be structured
108 according to local environmental variation (Morales *et al.* 2016a).

109 Previous studies have considered drivers of observed patterns of genetic and
110 phenotypic variation in EYR. Using microsatellites, nuclear intron sequences and one
111 mitochondrial gene, Pavlova *et al.* (2013) rejected three common explanations of
112 mitonuclear discordance based on selective neutrality (Toews & Brelsford 2012): (1)
113 inland-coast vicariance was not supported by models of past and present species
114 distributions, (2) incomplete lineage sorting was contradicted by the >1500 km extent
115 of the mitolineage contact zone and inferred nuclear gene flow between mitolineages,
116 and (3) male-biased dispersal is counter to known female-biased dispersal in EYR
117 (Debus & Ford 2012; Harrison *et al.* 2012). They found that maximum temperature
118 of the hottest month explains mtDNA variance over and above that explained by
119 geographic position and distance, which suggests environmental temperature as a
120 possible selective driver of mitolineage distribution (Fig. 1A). Pavlova *et al.* (2013)
121 concluded that the major nDNA north-south structure in EYR was consistent with
122 isolation-by-distance, and that inland-coastal mtDNA divergence occurred *in situ*.
123 Subsequently, Morales *et al.*, (2015) found evidence supporting selection on
124 mitochondrial genomes and confirmed extremely low mitogenome-wide intra-lineage
125 diversity consistent with selective sweeps. Morales *et al.* (2016a) expanded the
126 analysis of nDNA by analysing genome-wide neutral single nucleotide
127 polymorphisms (SNPs) and argued for the presence of two genetic populations,
128 northern and southern, with a zone of intergradation, modifying the previously
129 inferred isolation-by-distance. They also showed that plumage colour differentiation
130 follows a similar geographic trend, albeit with a broader zone of intergradation.
131 Reconstructions of the evolutionary histories of each genome are needed to better
132 understand mitonuclear discordance in EYR, an emerging model of mitonuclear
133 interactions and lineage divergence.

134 Here we propose a novel scenario to explain perpendicular mitonuclear
135 differentiation in EYR (Fig. 1C). Initial north-south divergence generated concordant
136 mtDNA and nDNA divergence, currently reflected in the major nDNA structure and
137 colour variation (first axis of differentiation) but not in mtDNA structure. Subsequently,
138 independent events of mitochondrial introgression might have occurred with little
139 associated nDNA introgression, one south-to-north coastwards of the Great Dividing
140 Range, and the other north-to-south inland of the Great Dividing Range.
141 Mitochondrial introgression would then have resulted in the current inland-coastal
142 mitochondrial split and inland-coast mitonuclear divergence-with-gene-flow in the
143 southern population (a second axis of differentiation). We used a coalescent
144 multilocus approach to explore this scenario by analysing 10 mitochondrial genes,
145 and 400 sequenced nuclear loci. We estimated nuclear divergence times, gene flow
146 rates and effective population sizes and tested whether the onset of mitochondrial
147 divergence coincided with north-south population divergence. We discuss our
148 findings in the context of adaptive mitochondrial evolution, introgression, and
149 mitonuclear co-evolution (Burton *et al.* 2013; Dowling *et al.* 2008; Gershoni *et al.*
150 2009; Hill 2015; Hill 2016).

151 **METHODS**

152 *Samples, molecular methods and datasets*

153 We analyzed (1) mitochondrial ND2 sequences, (2) 2728 SNPs and (3) phased
154 alleles for 400 nuclear sequences for 69 individuals, and (4) 10 mitochondrial genes
155 for 32 individuals (Fig. 1A-1B). Genomic DNA from 42 newly collected blood samples
156 was extracted with DNAeasy Kit (Qiagen, Germany) following the manufacturer's
157 protocol. For these samples, a partial region (~1000 bp) of mitochondrial ND2 gene
158 was amplified following Pavlova *et al.* (2013) and sequenced commercially
159 (Macrogen, Korea). The newly produced ND2 dataset was supplemented with
160 previously published ND2 sequences for 27 individuals (Genbank accession in
161 Table S1; Pavlova *et al.*, 2013). Based on ND2, all 69 individuals were assigned to
162 one of the two mitolineages (35 mito-A and 34 mito-B; Table S1; black and white
163 circles on Fig. 1A).

164 For the same 69 individuals, 1000 sequenced anonymous nuclear loci were
165 obtained by hybrid capture enrichment probes (size =240 bp; Lemmon *et al.* 2012).
166 Probe design, detailed in Appendix S1, was optimised using a draft of the EYR
167 genome (Morales, Wang, Pavlova and Sunnucks, unpublished data; sample code:
168 EYR056, Lat/Long: 143.41/-36.79). Briefly, DNA for genome sequencing was

169 prepared into one paired-end (500 bp insert size, 100 bp read length) and one mate-
170 pair (2 Kb insert size, 50 bp read length) library. Libraries were prepared and
171 sequenced with standard Illumina HiSeq™ 200 protocols at the Beijing Genome
172 Institute. The pair-end library produced 34,913 million bases and the mate-pair library
173 10,976 million bases. De novo assembly was performed with SOAPdenovo v1.05
174 with a K-mer size of 35 and default settings (Li *et al.* 2010). Capture probes included
175 sequenced regions with 40% and 55% GC content, low-copy number and with at
176 least 96% average identity across mapped reads. Probes were tiled uniformly at 2x
177 density (3 probes per locus) to form the probe set. Indexed libraries were prepared
178 from genomic DNA and enriched using an Agilent Sure Select enrichment kit.
179 Libraries were sequenced on an Illumina 2500 lane with paired-end 150 bp reads
180 and 8 bp indexing read.

181 The SNP dataset consisted of 2728 SNPs, previously used by Morales *et al.*
182 (2016a). They were obtained as follows: reads were mapped against the capture
183 probe references with BWA v. 0.7.12 (Li & Durbin 2009), PCR duplicates were
184 removed and InDel re-alignment was performed with Piccard v. 1.138
185 (<http://broadinstitute.github.io/picard/>). SNP-calling was performed with the
186 UnifiedGenotype in GATK v. 3.4 (DePristo *et al.* 2011). SNPs were filtered according
187 to Overall Quality ≥ 100 , Mapping Quality ≥ 20 , Depth ≥ 5 , Phred Score ≥ 20 ,
188 Heterozygosity ≤ 0.8 , Minor Allele Frequency ≥ 0.05 , and Genotype Frequency $\geq 90\%$.

189 The phased allele data set consisted of 400 nuclear sequences. Post-
190 processing of targeted captured loci including raw sequencing reads processing,
191 read assembly, orthology calculations and sequence alignment were performed
192 following Prum *et al.* (2015) (accompanying scripts can be found at
193 [doi:10.5281/zenodo.28343](https://doi.org/10.5281/zenodo.28343)). Allele phasing for each locus was determined
194 statistically from the assembled reads by drawing a posterior distribution for each
195 individual separately, following Pyron *et al.* (2016); for methodological details and
196 scripts see [doi:10.5061/dryad.51v22](https://doi.org/10.5061/dryad.51v22). In short, the method generates alleles with no
197 ambiguities for positions that can be phased with a $\geq 95\%$ posterior probability
198 confidence, leaving ambiguities for the remainder of the polymorphic sites. We
199 randomly selected 400 loci from the resulting phased alignments for coalescent
200 analyses (the maximum number of loci accepted by IMA2).

201 To appropriately assign inheritance scalars for the sequenced loci in the IMA2
202 analysis (below), we mapped the alignment consensus sequences to the Zebra
203 Finch *Taeniopygia guttata* genome taeGut3.2.4 (Warren *et al.* 2010) using BLASTn

204 v.2.3.0 (Camacho *et al.* 2009) with a E-value threshold of 1×10^{-4} (BLAST output doi:
205 10.6084/m9.figshare.3581004). Because historical inferences assume neutral
206 evolution of markers, we identified all nuclear loci that may have evolved under
207 directional selection (outlier loci) and removed them from SNP and sequenced
208 marker datasets. Outlier loci were identified with LOSITAN (Antao *et al.* 2008) with
209 samples divided into 10 populations based on their geographic location (Fig. 2B). All
210 the data used in this project (capture probes for the EYR hybrid capture enrichment,
211 raw reads, and phased sequence alignments) have been deposited in figshare
212 (doi:10.6084/m9.figshare.3581004) and SRA (accession: SRP079228) online digital
213 repositories.

214 Sequences of 10 protein-coding mitochondrial genes (ND1, ND2, ND3, ND5,
215 ND6, COX1, COX2, COX3, ATP6 and ATP8) were extracted from 32 published
216 mitogenome sequences (14 mito-A and 18 mito-B, represented by stars on Fig. 1A;
217 Genbank accessions in Table S2; Morales *et al.*, 2015). These genes were chosen
218 because they did not show signatures of positive selection between mitolineages
219 (Morales *et al.* 2015).

220 *Nuclear DNA genetic structure*

221 We used the SNP dataset and admixture model with correlated allele frequencies
222 implemented in STRUCTURE 2.3.4 (Pritchard *et al.*, 2000) to confirm the presence
223 of major and minor nDNA structure and assign each individual to one of three
224 populations (northern, south-inland and south-coast: red, light blue and dark blue on
225 Fig. 1C, respectively) for IMA2 analysis (below). To meet STRUCTURE assumptions
226 that loci are in linkage and Hardy-Weinberg equilibrium (HWE), we (a) subsampled
227 one SNP per locus (i.e. per capture probe) and (b) filtered out loci not in HWE with
228 the HWE.test.genind function in the R package adegenet 2.0.0 (Jombart & Ahmed
229 2011; R Development Core Team 2014). The initial significance level ($\alpha < 0.05$) of
230 the HWE test was corrected for multiple tests using the B-Y method to account for
231 False Discovery Rate (FRD < 1%) following Narum (2006). To reduce Wahlund effect,
232 which could cause loci to be falsely concluded to deviate from HWE through non-
233 Mendelian inheritance, samples were divided into 10 populations based on their
234 geographic location (Fig. 2B from the main text). The filtering process resulted in a
235 reduced dataset of 706 SNPs. STRUCTURE analyses were performed assuming 1
236 to 5 genetic populations (K) with 25 independent Markov chains of 200,000 iterations
237 of burn-in and 80,000 recorded iterations for each K . Convergence of the parameters
238 alpha and Log-Likelihood across chains was determined for every K value with

239 custom R scripts (Gonçalves da Silva, 2016;
240 <https://zenodo.org/record/48790#.V3KiXZN96Rs>). Results were summarized and the
241 optimal number of populations estimated with the Evanno test (Evanno *et al.* 2005) in
242 STRUCTURE HARVESTER Web v0.6.94 (Earl 2012). Average Q-values across
243 replicates were obtained with CLUMPP v 1.1.2 (Jakobsson & Rosenberg 2007).
244 Individuals with a posterior probability (Q-values) of ≥ 0.8 of belonging to a particular
245 population were assigned to that genetic population.

246 ■ We used discriminant analysis of principal components (DAPC: Jombart *et al.*
247 2010) implemented in adegenet to estimate the amount of genetic variation
248 explained by the major and minor axes of nDNA structure. The DAPC analysis was
249 conducted with 10 populations delimited based on their geographic location (Fig. 2B).
250 To estimate the number of loci contributing to the observed nDNA genetic structure
251 we performed a pairwise Nei's G_{ST} (Nei 1973) test between samples unambiguously
252 assigned to populations by STRUCTURE (i.e. assignment probability of $Q > 0.8$ from
253 $K=3$ STRUCTURE analysis, see Results) using the same unlinked 706 SNPs. We
254 created genind objects for each pairwise comparison with the R package adegenet
255 (Jombart & Ahmed 2011) and 1000 bootstrap samples, with each subpopulation
256 resampled according to its size, with the function `chao_bootstrap` of the `mmod` R
257 package (Winter 2012). Then, for each set of permuted dataset we obtained the
258 observed per-locus Nei's G_{ST} value and its normalized 95% Confidence Intervals (CI)
259 (i.e. centered on the observed value and corrected with standard deviation across
260 replicates) with the function `summarise_bootstrap` in `mmod`. Loci were considered
261 significantly differentiated if the lower bound of the CI was greater than zero.

262 *Isolation-with-migration models*

263 To estimate times of population divergence, gene flow and effective population sizes,
264 we fitted a three-population model of isolation-with-migration (Hey & Nielsen 2004)
265 implemented in IMA2 (Hey 2010) to the multilocus dataset comprising sequences of
266 400 randomly-selected anonymous nuclear loci. For each locus, the longest stretch
267 of each sequence without ambiguities was used. Recombination points were
268 detected for each locus with the program IMgc (Woerner *et al.* 2007) and the longest
269 non-recombining block was retained. Resulting alignments had lengths from 124 to
270 529 bp (mean = 264 bp). IMA2 estimates model parameters scaled by mutation rate
271 (μ), population divergence time in generations ($t = t\mu$), migration rate ($m = m/\mu$) and
272 effective population sizes ($\theta = 4N_e\mu$). Inheritance scalars were set to 1.0 for
273 autosomes and 0.75 for Z-linked loci.

274 In order to estimate historical gene flow between three largely panmictic
275 populations, we subsampled “pure” individuals from each population (based on
276 $Q > 0.8$ from $K=3$ STRUCTURE analysis), avoiding admixed individuals from
277 contemporary hybrid zones. Individuals with a posterior probability (Q-values) of
278 population membership < 0.8 were not used in the analysis because they could not
279 be assigned to any population unambiguously, and arbitrary assignment would
280 inevitably add stochasticity to the divergence estimates. As a result, we have likely
281 underestimated gene flow among contemporary populations. We accepted this
282 compromise because precise estimates of divergence were essential whereas
283 slightly imprecise estimates of gene flow were acceptable given our aims. Moreover,
284 to avoid excessive IMA2 computation time inherent to analyses with very large
285 numbers of loci, we further subsetted the dataset by randomly selecting individuals
286 from the “pure” populations (northern: $N=9$ individuals, 18 alleles, southern inland:
287 $N=7$ individuals, 14 alleles, and southern coastal: $N=8$ individuals, 16 alleles, Table
288 S1; Fig. 1B). Sixteen parameters were estimated: two of t , eight of m and six of θ (θ s
289 were estimated at three time intervals: t_1 , t_0 and present; model option j5; see
290 legend of Fig. 3A). Multiple preliminary analyses were run to optimize prior parameter
291 boundaries. Eight independent replicates were run for the final analysis, each
292 involved $> 11 \times 10^6$ steps after a burn-in period of $> 4.8 \times 10^5$ steps, employing 150
293 MCMC chains with geometric heating (parameters $a = 0.999$ and $b = 0.3$). Parameter
294 estimates were converted to demographic units using a generation time of 3.5 years
295 (Pavlova *et al.*, 2013) and a mutation rate of 1.2×10^{-9} (lower bound = 0.7×10^{-9} ;
296 upper bound = 2.5×10^{-9}) nucleotides per base per year, which have been used to
297 estimate demographic parameters in passerines (Ellegren 2007; Lee & Edwards
298 2008). The mutation rates we used incorporate a wide range of values that have
299 been previously to capture most rates of slow-evolving introns (Ellegren 2007) and of
300 faster-evolving anonymous loci (Lee & Edwards 2008). Moreover, this conservative
301 approach allows IMA2 to directly infer per-locus mutation rates from a wide range of
302 prior values.

303 *Mitochondrial lineage divergence*

304 To test for simultaneous divergence of mitolinesages (mito-A and mito-B) and nuclear
305 DNA, we built a calibrated phylogeny in BEAST v.1.8.0 (Drummond *et al.* 2012)
306 using sequences of 10 protein-coding mitochondrial genes that are free from
307 signatures of positive selection. Although mitolineage divergence time was estimated
308 previously from ND2 (1.5 (0.98–2.15) million years ago (MYA); Pavlova *et al.*, 2013),
309 by using multiple genes we improve the precision of the estimate. The optimal

310 partitioning scheme and substitution models were identified using PartitionFinder
311 (Lanfear *et al.* 2012; Table S3). Linked trees, linked clock models, and unlinked
312 substitution models were used. We performed four replicates with 8×10^7
313 generations sampled every 2000 steps after 10% of burn-in. The four independent
314 runs were combined and convergence checked in Tracer v1.6.0 (Rambaut *et al.*
315 2014). Mitolineage divergence time was calibrated assuming neutral evolution rates
316 for mitochondrial genes of the Hawaiian honeycreeper (Lerner *et al.* 2011). In order
317 to translate honeycreeper mutation rates to the EYR we assume that rates among
318 passerines should be similar, that strong purifying selection acting on the EYR
319 mitogenome should also act on the honeycreeper mitogenome, and that we prevent
320 major bias of diversifying selection by avoiding genes with evidence of positive
321 selection (Morales *et al.*, 2015)

322 **RESULTS**

323 *Nuclear DNA genetic structure*

324 The STRUCTURE models with two and three populations ($K = 2$: $\text{LnP}(K) = -$
325 38224.17 ; $\Delta K = 217.1$ and $K = 3$: $\text{LnP}(K) = -37503.8$; $\Delta K = 225.9$) reached
326 convergence for all chains (Figs. S1-S2). These supported two main populations
327 (northerly and southerly) with some individuals displaying intermediate assignment
328 scores (red and blue in Fig. 1B and Fig. 2A; Table S1). The higher likelihood model
329 assuming $K = 3$ (Fig. S3) further sub-divided the southern population into inland and
330 coastal populations, in which all inland individuals ($Q > 0.8$) belong to mito-A
331 mitolineage, and coastal individuals to mito-B mitolineage (shades of blue in Fig. 1B
332 and Fig. 2A). $K = 4$ and $K = 5$ analyses did not show any additional geographically
333 meaningful structure (not shown). DAPC showed that 48% of genetic variation is
334 explained by the major north-south structure (PC1 on Fig. 2C), and 12% is explained
335 by the minor southerly inland-coast structure (PC2 on Fig. 2C). The number of
336 polymorphic loci considered for the pairwise G_{ST} test was as follows: north vs. south-
337 coastal = 574; north vs. south-inland = 628; south-inland vs. south-coastal = 605.
338 Mean pairwise G_{ST} estimates were low to medium for all population comparisons;
339 mean G_{ST} (mean 95% CI): north vs. south-coastal = 0.09 (0.02-0.18); north vs.
340 south-inland = 0.07 (-0.03-0.19); south-inland vs. south-coastal = 0.04 (-0.02-0.11).
341 The two north-south comparisons had more significantly differentiated SNPs than the
342 comparisons between the southern populations: north vs. south-coastal = 284 SNPs
343 (49%); north vs. south-inland = 188 SNPs (30%); south-inland vs. south-coastal =
344 141 SNPs (23%) (Fig. S4).

345 *Population divergence: isolation-with-migration model*

346 Convergence of IMa2 parameter estimates was confirmed by lack of trends on
347 parameter plots, similarity of estimates across replicate and appropriate mixing of
348 chains (low parameter autocorrelation; mean = 0.013). Posterior parameter
349 distributions were contained within the bounds of the prior distributions for all
350 parameters, except for migration from the southern to the northern ancestral
351 population (Fig. S5). At least 11,000 genealogies were recorded for each of the eight
352 replicate runs.

353 IMa2 (Fig. 3A; Table S4) placed divergence between northern and southern
354 populations in the late Pliocene or early Pleistocene (high point $t_1=2,380,269$; 95%
355 highest posterior density [HPD] 1,941,225 – 3,002,718 years ago), and the split
356 between southern inland and southern coastal populations in the late Pleistocene
357 ($t_0=64,435$; 21,812 – 118,244 years ago). Compared to the ancestral effective
358 population size ($N_{e_{ANC}}=85,688$; 34,700 – 13,6676), sizes of southern ($N_{e_S}=488,098$;
359 398,317 – 667,801) and northern ($N_{e_{N1}}=424,677$; 305,779 – 771,158) populations
360 grew after t_1 , but declined dramatically after t_0 in all three descendant populations:
361 southern coastal ($N_{e_{SC}}=23,369$; 12,039 – 47,447), southern inland ($N_{e_{SI}}=29,035$;
362 14,871 – 53,112) and northern ($N_{e_{N2}}=242,901$; 138,092 – 626,727) (Fig. 3A; Table
363 S4). Even though gene flow was likely under-estimated due to omitting admixed
364 individuals from the IMa2 analysis, our results showed non-zero nuclear gene flow
365 between all ancestral and all current genetic populations (Fig. 3A; Table S4). For the
366 t_1 -to- t_0 time period, forward-in-time gene flow from south to north ($m_2=5.8$; 4.2 – 9.4)
367 was higher than that from north to south ($m_1=0.4$; 0 – 1.5). For t_0 -to-present, gene
368 flow from southern to northern populations ($m_4=5.3$; 1 – 7.8, $m_8=0.7$; 0.4 – 0.9) was
369 higher than that from northern to two southern ones ($m_3=1.6$; 0.7 – 2.4, $m_7=4.5$; 1 –
370 6.8), and gene flow from coast to inland ($m_6=3.8$; 2.5 – 5.4) was higher than that
371 from inland to coast ($m_5=1.02$; 0.2 – 1.5). These nuclear gene flow estimates
372 suggest that neutral gene migration was primarily in the south-to-north direction.

373 *Mitochondrial lineage divergence*

374 Convergence for the combined BEAST run of the 10 protein-coding mitochondrial
375 gene dataset was confirmed with trend plots and high effective sample sizes (>2000)
376 for all parameters. The mitochondrial tree reflects the known deep mitochondrial split
377 between mito-A and mito-B, and when compared to the nDNA structure also reflects
378 the known strong mitonuclear discordance (Fig. 4). Mitolineages mito-A and mito-B
379 were estimated to have diverged in the late Pliocene or early Pleistocene (2,000,000;

380 1,700,000 - 2,400,000 years ago; Fig. 4; Table S4). These dates overlap with the
381 95%HPD of the time of population divergence between northern and southern
382 populations, and thus consistent with the prediction that mitochondrial and nuclear
383 divergence coincided temporally. The time to the most recent common ancestor
384 (TMRCA) for mito-A was placed in the mid Pleistocene (276,000 – HPD: 213,000 –
385 319,000 years ago) and TMRCA for mito-B in the late Pleistocene (90,000 – HDP:
386 56,000 – 96,000 years ago). These times are recent relative to the divergence time
387 between mitolineages (Fig. 3B; Fig. 4), presumably because the inland and coastal
388 mitochondrial selective sweeps occurred at these times (Rambaut *et al.* 2008;
389 Thomson *et al.* 2000).

390

391 **DISCUSSION**

392 We explored whether evolution of mitonuclear discordance in the EYR could be
393 explained by a model of two independent events of mitochondrial introgression
394 leading to perpendicular axes of nuclear and mitochondrial genetic differentiation (Fig.
395 1C). Coalescent analyses provided evidence of temporally concordant nDNA and
396 mtDNA divergence. This strongly supports our hypothesis that EYR mitonuclear
397 discordance was caused by population divergence followed by two independent
398 events of mitochondrial introgression. Mitochondrial lineage divergence and
399 introgression generated a deep inland-coastal mitochondrial split within each of the
400 two divergent nuclear genetic backgrounds (north and south; Fig. 1C). One plausible
401 driver of this major shift is adaptive mitochondrial introgression during a period of
402 transition from relatively warm, stable climates with high summer precipitation, to
403 more variable and winter-dominated rainfall climates, and aridification of inland
404 Australia (below) (Byrne *et al.* 2011; Byrne *et al.* 2008; Hocknull *et al.* 2007;
405 Sniderman *et al.* 2009). This process could have had implications for mitonuclear co-
406 introgression because divergent inland-coastal mitochondrial types would need to
407 maintain mitonuclear interactions suitable for metabolic functioning under local
408 environmental variation (Morales *et al.* 2016b). Overall, our data suggest that a first
409 axis of differentiation was formed during north-south divergence-with-gene-flow
410 (reflected in plumage colour subspecies and major nDNA structure, Morales *et al.*
411 2016a and this paper), and was supplemented by a second perpendicular axis of
412 differentiation during two events of mitochondrial introgression generating inland-
413 coast mitochondrial divergence-with-gene-flow (consistent with two deeply divergent
414 mitolineages).

415

416 *Eastern Yellow Robin evolutionary history*

417 The geographic pattern of nDNA, colour variation and mtDNA in EYR indicate that
418 the concordant early-Pleistocene divergence of mtDNA and nDNA occurred in the
419 north-south direction. This is reflected in present-day distributions of nDNA and
420 plumage colour being structured north-south (Fig. 1B; Morales *et al.* 2016a).
421 Mitolineage mito-A is the only population currently occurring in the northern part of
422 the species' range and it shows evidence of late-Pleistocene intra-lineage vicariance
423 between the northernmost part of its range and the rest of the mitolineage (Fig. 1A;
424 Fig. 4). Large-scale Pleistocene climatic shifts are likely drivers of the initial north-
425 south divergence (Byrne *et al.*, 2008; 2011). Two vicariant/environmental barriers
426 located near the zone of intergradation between northern and southern populations
427 could have facilitated north-south EYR divergence (Fig. 1B). The Hunter Valley
428 Barrier is a dry lowland river valley with low vegetation density that started to form
429 with the opening of the Sydney Basin during the early Permian (~299 Ma) and
430 continued to be shaped until more recent times with sea levels changes during the
431 Pleistocene (Boyd & Roy 1995; Percival *et al.* 2012). The Southern Transition Zone
432 is a region between lowlands and highlands of the central Great Dividing Range that
433 experience intermittent periods of glaciation and pre-glaciation during the Pleistocene
434 (Barrows *et al.* 2002). These two barriers have been implicated in subspeciation in
435 several bird species and other closed-forest taxa including invertebrates, lizards,
436 frogs, mammals and plants (Bryant & Krosch 2016; Ford 1987; Schodde 2006;
437 Schodde & Mason 1999).

438 Given the clear pattern of north-south historical divergence, we can explain
439 the current mitonuclear discordance in EYR by invoking two instances of long-range
440 introgression of mitolineages that became fixed with little associated nuclear
441 introgression (Fig. 1C). Estimating with certainty where in space the initial north-
442 south divergence occurred is not possible, because any number of demographic
443 events could have overwritten the genetic signal of population structure. However,
444 two lines of evidence support the contention that divergence occurred somewhere in
445 the vicinity of the current north-south contact zone (Fig. 1B). First, hundreds of
446 genome-wide genetic markers support divergence at this region (Fig. S4). Second,
447 previous geographic cline analyses showed that genetic and plumage colour clines
448 have their centre estimates (i.e. maximum rate of frequency change) at the contact
449 zone, suggesting that colour evolution is a by-product of neutral genetic divergence

450 that occurred close to this geographic region (Morales *et al.* 2016a). Accepting the
451 population scenario just described, we can infer the direction and time of
452 introgression by the geographic positions of mitolineages and the estimated time of
453 mitochondrial sweeps (Fig. 1C; Fig. 3B). The data can be explained if northern mito-
454 A introgressed southwards along the inland side of the Great Dividing Range in the
455 mid Pleistocene, while southern mito-B introgressed northwards along the coast in
456 the late Pleistocene. Thereafter, in the southern population only, nDNA is inferred to
457 have sorted into coastal and inland populations, concordant with the mitochondrial
458 split (Fig. 1; Fig. 3A).

459

460 *Mitochondrial DNA introgression was likely adaptive*

461 Showing conclusive evidence of fitness effects of mtDNA introgression in wild
462 populations is challenging. First steps towards demonstrating adaptive nature of
463 mtDNA introgression, however, come from rejecting scenarios of neutral
464 introgression and strong genetic evidence of non-neutral evolution (Ballard & Melvin
465 2010; Boratyński *et al.* 2014; e.g. Doiron *et al.* 2002; Llopart *et al.* 2014). Our current
466 data do not provide for a definitive test for adaptive mitochondrial introgression, but
467 several major patterns in the data are not congruent with selectively-neutral
468 scenarios.

469 Empirical data for birds with female-biased dispersal overwhelmingly show
470 very little mitochondrial flux between hybridizing lineages in a range of contact
471 scenarios, consistent with the theoretical expectation of relatively low mitochondrial
472 flow between taxa with female-biased dispersal (Currat *et al.* 2008; Petit & Excoffier
473 2009; Rheindt & Edwards 2011; Toews & Brelsford 2012). The migration parameter
474 estimates here and the data in Morales *et al.* (2016a) indicate that gene flow
475 occurred during north-south divergence of EYR. However, we cannot clearly
476 distinguish among alternative models of divergence: secondary contact, primary
477 intergradation and spatial invasion. Thus, interpreting mtDNA vs. nDNA introgression
478 in terms of different population divergence scenarios is complicated (Petit & Excoffier
479 2009). Despite this limitation, our data is not consistent with neutral introgression
480 under female-biased dispersal. We argue this is because EYR underwent complete
481 mitochondrial replacement with little associated nuclear gene flow over large
482 proportions of the species' range. Further, this occurred in two opposing directions
483 and was correlated with contrasting climates.

484 Our data on EYR do not agree with non-adaptive explanations for high
485 mitochondrial introgression based on unequal or small effective population sizes and
486 mutation load (Sloan *et al.* 2016; Toews & Brelsford 2012). This is because our
487 coalescent estimates show that ancestral populations had equally large population
488 sizes. We cannot reject outright another class of explanation for high mtDNA flow
489 relating to higher female dispersal (Petit *et al.* 2004) and propensity to mate with
490 available males (Roca *et al.* 2005) as a possible driver of neutral mitochondrial
491 introgression in the north-south direction. However, EYR is among the more
492 sedentary of birds, typically dispersing less than a few kilometres (Amos *et al.* 2014;
493 Debus & Ford 2012; Harrisson *et al.* 2012). Also, the sexes in EYR are very similar in
494 size and appearance and live in territorial pairs, indicating that the mating system is
495 likely to be approximately monogamous and not particularly disposed to
496 exceptionally female-biased gene flow (Higgins & Peter 2002). On balance, we
497 consider that female-biased dispersal alone is implausible as an explanation of
498 inferred mitochondrial introgression in EYR over hundreds of kilometres.

499 In summary, EYR mitochondrial introgression cannot be explained exclusively
500 by selectively neutral explanations: (1) mitochondrial introgression events in EYR
501 resulted in two cases of near-fixation through large geographic expanses of
502 contrasting environments, in opposite latitudinal directions, accompanied with little
503 signal of nDNA introgression, and (2) such patterns are anticipated by evidence of
504 adaptive mitochondrial evolution (selective sweeps, and amino acids in genes
505 plausibly connected the climate adaptation showing signals of positive selection) in
506 this system (Morales *et al.* 2015; Fig. 1; Pavlova *et al.* 2013).

507 A model of adaptive mitochondrial introgression can explain the demographic,
508 ecological and evolutionary features of EYR introgression history. We propose that
509 first, large ancestral northern and southern population sizes could have promoted the
510 accumulation of adaptive mitochondrial variation in each lineage (Fig. 3A; Table 1;
511 Camus *et al.* 2015; Kimura *et al.* 1963; Ohta 2002). Later, adaptive alleles could
512 have fully replaced alternative mitochondrial alleles in response to large-scale
513 climatic change, generating the observed mitochondrial selective sweeps in each
514 mitolineage (Byrne *et al.* 2011; Byrne *et al.* 2008; Rheindt & Edwards 2011;
515 Rieseberg 2009). This model of adaptive mitochondrial introgression holds
516 regardless of the assumed spatial model of divergence, and instead depends on
517 large effective population sizes and strong environmental contrasts between inland
518 and coastal regions. Mitochondrial adaptive evolution could have been essential to
519 meet metabolic requirements under differential environmental conditions, leading to

520 increased rates of heat production in colder environments and decreased
521 heat/increased rates of energy production in warmer environments and/or during
522 caloric restriction in drier environments (Das 2006; Wallace 2005). Testing metabolic
523 consequences of introgression requires data on fitness responses to environmental
524 variation and hybridization (e.g. Boratyński *et al.* 2016; Pereira *et al.* 2014).

525

526 *Perpendicular axes of differentiation in the Eastern Yellow Robin*

527 The most striking and unexpected pattern in Eastern Yellow Robin is that of
528 perpendicular axes of differentiation in which nuclear variation is structured north-
529 south and mitochondrial variation east-west (Fig. 1). Mitonuclear interactions are
530 obvious candidates to be both causes and consequences of the observed population
531 genetic patterns. The strong fitness consequences of mitochondrial DNA variation
532 (Wolff *et al.* 2016) are likely to be amplified through mitonuclear co-evolution of
533 essential metabolic and physiological functions (Bar-Yaacov *et al.* 2012; Boratyński
534 *et al.* 2016; Deremiens *et al.* 2015). On the other hand, disrupted mitonuclear
535 interactions can form strong, long-lasting barriers to gene flow and promote
536 speciation (Burton *et al.* 2013; Dowling *et al.* 2008; Gershoni *et al.* 2009; Hill 2015;
537 Hill 2016). In EYR, one possible explanation for the dramatic reduction of effective
538 population sizes in all three populations at (t_0) after the onset of mitochondrial
539 introgression is strong selection against hybrids bearing incompatible mitonuclear
540 combinations (Fig. 3). Evidence from laboratory crosses across a wide range of
541 animal systems shows that mitonuclear incompatibility fitness effects in hybrids
542 include metabolic malfunctioning, low fertility and increased mortality (reviewed in
543 Burton *et al.* 2013; Levin *et al.* 2014).

544 The common observation of mitonuclear incompatibilities raises the question
545 of how mitochondria in EYR were able to introgress swiftly into divergent genomic
546 backgrounds. A likely explanation is that mitonuclear interactions resulting from
547 introgression were maintained through mitonuclear co-introgression (Beck *et al.*
548 2015). Morales *et al.* (2016b) offers genomic data to support this idea: genome-wide
549 differentiation between coastal and inland populations is concentrated in a ~15.6 Mb
550 region of the genome enriched for nuclear-encoded genes with mitochondrial
551 function that co-introgressed with mitogenomes to maintain locally adapted
552 mitonuclear interactions. Behavioural, metabolic and physiological experiments are
553 required to explore the mechanism by which coastal and inland populations maintain
554 their mitonuclear divergence (e.g. Boratyński *et al.* 2016; Hill & Johnson 2013;

555 McFarlane *et al.* 2016). One set of predictions arise from the hypothesis that birds
556 from mitonuclear lineages should be able to recognize each other and mate
557 assortatively (i.e. the mitonuclear sexual selection hypothesis; Hill & Johnson 2013).

558 Despite the large amount of data amassed for EYR, it remains unclear
559 whether either or both of the perpendicular axes of differentiation will lead to
560 speciation. Our data show the importance of understanding phenotypic and
561 mitonuclear diversity patterns before arriving at taxonomic conclusions. Speciation is
562 a complex process that operates along a continuum, and under the biological
563 species concept, the trajectory towards full speciation in EYR seems to be impeded
564 for now (Seehausen *et al.* 2014; Shaw & Mullen 2014). The real challenge for
565 taxonomy then may be that of upon which criteria one can meaningfully, or indeed
566 whether one should, diagnose any intraspecific populations e.g., on plumage and
567 nDNA, or on mtDNA. On the other hand, biological and conservation implications of
568 EYR intraspecific variation are clearer: evidence for natural selection operating in
569 different directions and evidence for restricted gene flow on historical timescales
570 indicate that EYR populations are genetically and ecologically non-exchangeable
571 (Crandall *et al.* 2000).

572

573 *Drivers of differentiation in Eastern Australia*

574 Detailed reconstruction of Quaternary climates in Australia is limited by a paucity of
575 suitable fossil sites, a relatively narrow range of modern climate space for calibration,
576 and large regional variability (Hocknull *et al.* 2007; Porch 2010; Saltré *et al.* 2016;
577 Sniderman 2011; Sniderman *et al.* 2009). However, there is consensus on key
578 paleoclimatic phenomena that could have driven perpendicular differentiation in EYR.
579 The most important of these are: (i) a major transition in the early Pleistocene from
580 relatively warm, stable climates with high summer precipitation, to later more variable
581 ones characterized by winter-dominated rainfall and, (ii) major differences between
582 northern and southern Australia in the severity and timing of increased summer
583 aridity, and (iii) more severe aridity inland than on the coast (Byrne *et al.* 2011; Byrne
584 *et al.* 2008; Hocknull *et al.* 2007; Sniderman *et al.* 2009).

585 Multiple lines of evidence indicate that warm and moist early-Pleistocene
586 climates in Australia persisted until transition to modern winter-dominated rainfall
587 (Sniderman *et al.*, 2009). These conditions are likely to have applied broadly across
588 south-eastern Australia, and would have been in place during our proposed phase of
589 north-south divergence of EYR. The adaptive introgression that we propose would

590 have occurred during a transition from the mild early-Pleistocene climate to more
591 variable climates with winter-dominated rainfall and summer aridity. This period of
592 climate change involved considerable temporal and spatial complexity, such as
593 oscillation between wetter and drier vegetation types and multiple periods of rapid fall
594 in humidity and temperature (Hocknull *et al.* 2007; Saltré *et al.* 2016; Sniderman
595 2011; Sniderman *et al.* 2009). However, it is clear that this shift occurred later in
596 northern Australia than in the south: a north-eastern tropical rainforest fauna 500-280
597 KYA was replaced by a xeric fauna 205-170 KYA, while the south experienced
598 increasing aridity from as early as 600 KYA (Hocknull *et al.*, 2007). In addition, due to
599 the rain-shadow effect of the Great Dividing Range, aridity is more severe inland than
600 on the coast. This pattern also likely developed earlier in southern than northern
601 Australia (Hocknull *et al.*, 2007).

602 We predict that many co-distributed species may have been impacted
603 similarly by these widespread paleoclimatic events. If adaptive mitochondrial
604 introgression is common in the Australian avifauna (e.g. Kearns *et al.* 2014; Shipham
605 *et al.* 2015, 2016), then that, coupled with strong shifts in climate-related selective
606 forces, could provide a general explanation for the very high rate (~ 50%) of
607 mitochondrial paraphyly observed in Australian birds (Joseph & Omland 2009).
608 Accordingly, strong shifts in environmental gradients associated with paleoclimatic
609 cycling could also be a common general mechanism for mitonuclear co-evolution as
610 a driving force in generating genomic conflict and mitonuclear speciation (Hill 2015).
611 Whether similar phenomena have occurred in other taxa, and on other continents
612 with suitable conditions, demands further investigation of evolutionary impacts and
613 biodiversity implications of Quaternary climate change.

614

615 **Acknowledgements:**

616 Funding was provided by Australian Research Council Linkage Grant (LP0776322) and the
617 Holsworth Wildlife Research Endowment (2012001942). HM was funded by a Monash
618 University with a Graduate Scholarship (MGS), a Faculty of Science Dean's International
619 Postgraduate Research Scholarship, and a Postgraduate Publication Award (PPA) and by the
620 Department of Public Education (SEP) of the Mexican Government. Bioinformatic analyses
621 were undertaken using the Monash Sun Grid high-performance computer facility. We are
622 grateful to Philip Chan for technical support. Field samples were collected for this study
623 under scientific research permits issued by the Victorian Department of Environment and
624 Primary Industries (numbers 10007165, 10005919 and 10005514) and New South Wales

625 Office of Environment and Heritage (SL100886). We thank Nevil Amos and Richard Major
626 for coordinating the fieldwork and Holly Sitters and Christine Connelly for providing genetic
627 samples from South and East Victoria. We thank Anders Gonçalves da Silva and Biao Wang
628 for inputs regarding data analysis, and Kaspar Delhey for valuable discussions that helped to
629 improve the manuscript. We thank Scott Edwards, Mike Webster, Lynna Kvistad and
630 Stephanie Falk for valuable comments on the manuscript. We are grateful to three anonymous
631 reviewers and editor Matthew Miller from Axios Review for helpful comments on the first
632 draft of this manuscript, and Karen Chambers, Frederic Austerlitz and four anonymous
633 reviewers during the *Molecular Ecology* review process. The authors are also grateful to
634 Alan Lemmon for coordinating the hybrid capture sequencing project.

635

FIGURES

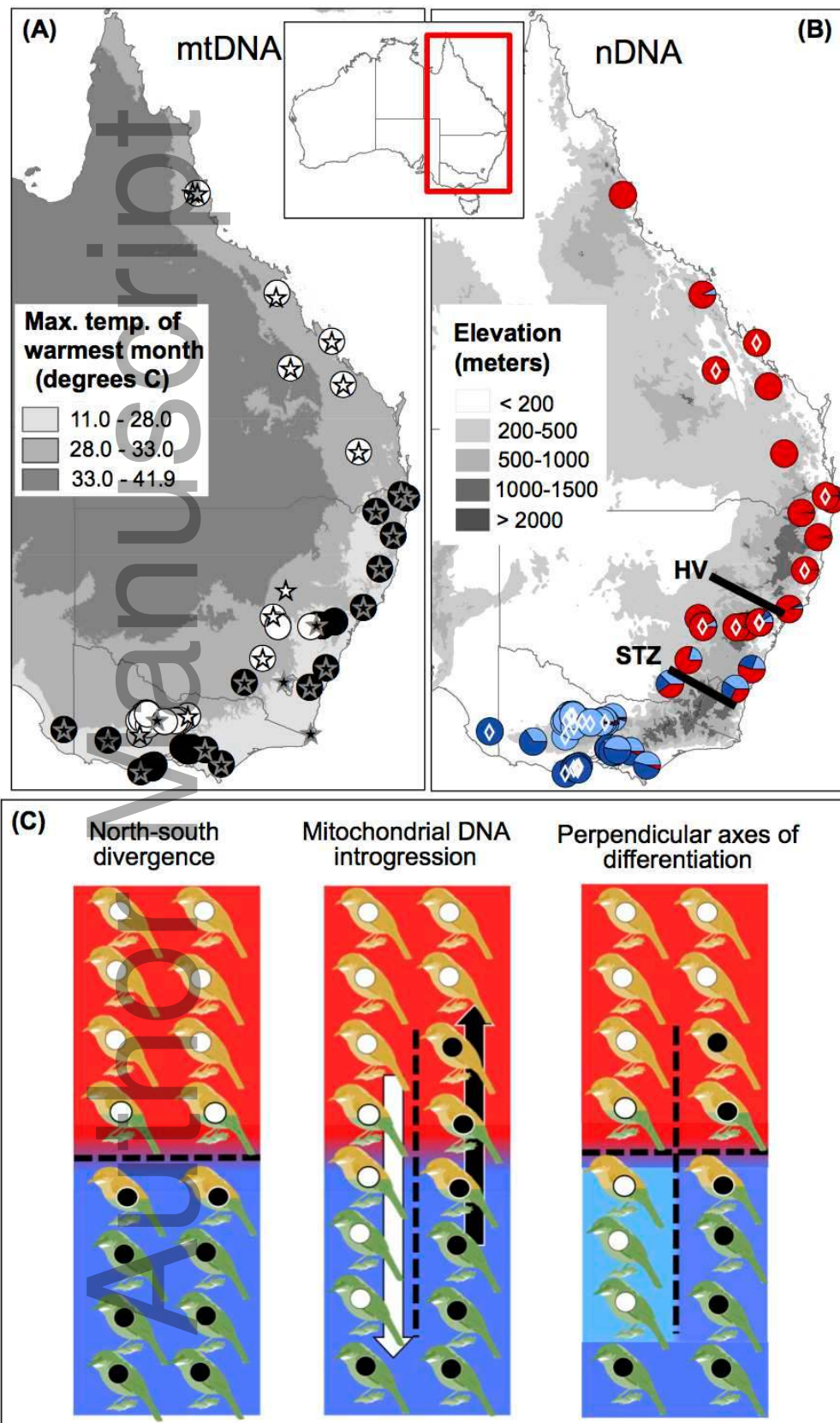


Figure 1 Distribution of Eastern Yellow Robin samples used in this study showing their contribution to mitochondrial (A) and nuclear (B) genetic structures and a schematic representation of EYR evolutionary history (C). (A). Distribution of mitochondrial lineages mito-A (white) and mito-B (black) plotted over the maximum temperature of the warmest month. Circles represent samples sequenced for the mitochondrial ND2 gene, stars-samples for which data from 10 mitochondrial genes were used. (B) Distribution of samples for which nuclear loci were sequenced, mapped over elevation map featuring the Great Dividing Range (dark shading); pies show individual membership in three genetic populations according to $K=3$ STRUCTURE analysis (see Fig. 2A): northern population (red), southern coastal population (dark blue) and southern inland population (light blue). Samples used for IMA2 analysis are indicated with white diamonds. Black lines represent potential vicariant/environmental barriers, HV- Hunter Valley and STZ- Southern Transition Zone. (C) Evolutionary history of the Eastern Yellow Robin, the colours of the boxes represent their nuclear genomic background (colour of the background; north = red and south = blue), their plumage colouration (colour of the birds; northern yellow, southern green and intermediates of mixed colour), and their mitochondrial membership (colour of the circles; mito-A = white and mito-B = black). First panel shows the first axis of differentiation: mtDNA, nDNA and colour differentiation between northern and southern birds with a zone of intergradation. The second panel shows the second axis of differentiation: two independent events of mitochondrial introgression occurred without nDNA introgression, resulting in mtDNA genetic structure in the inland-coastal direction. The third panel shows the current perpendicular pattern of differentiation: inland-coast mitochondrial divergence in the face of nuclear gene flow, major north-south nDNA structure and plumage colouration divergence and a minor inland-coast nuclear DNA divergence in the southern range (shades of blue).

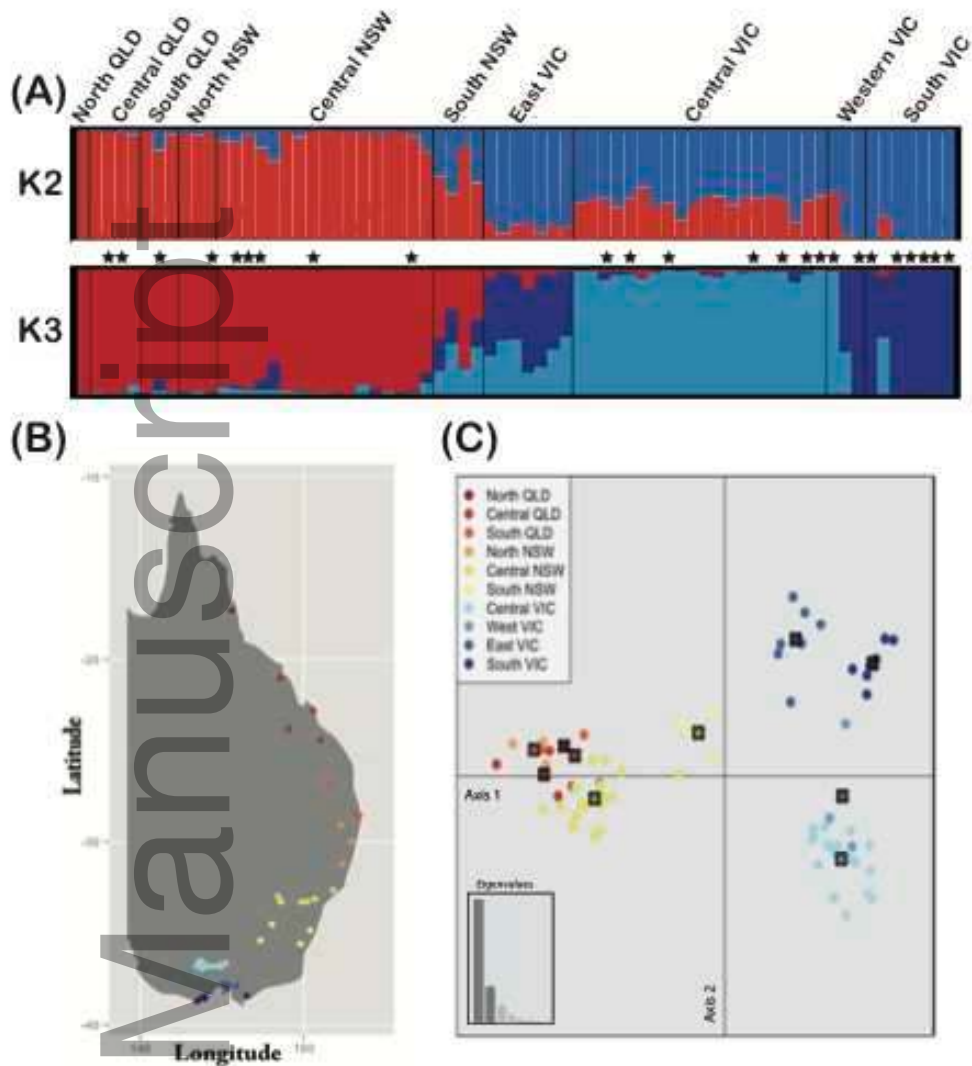


Figure 2 Summary of population genetic structure in the Eastern Yellow Robin. (A) The results of STRUCTURE (Pritchard *et al.* 2000) models when $K = 2$ and $K = 3$. Results were summarised with STRUCTURE HARVESTER Web v0.6.94 (Earl 2012) and CLUMPP v 1.1.2 (Jakobsson & Rosenberg 2007). Samples used for IMA2 analysis are indicated with black stars. (B) Map of samples used for the nuclear DNA data arranged into arbitrary populations according to geographic position. (C) Discriminant Analysis of Principal Components (DAPC; Jombart *et al.* 2010) for populations from panel B, axis 1 (PC1) captured 48% of genetic variation and axis 2 (PC2) captured 12% of genetic variation.

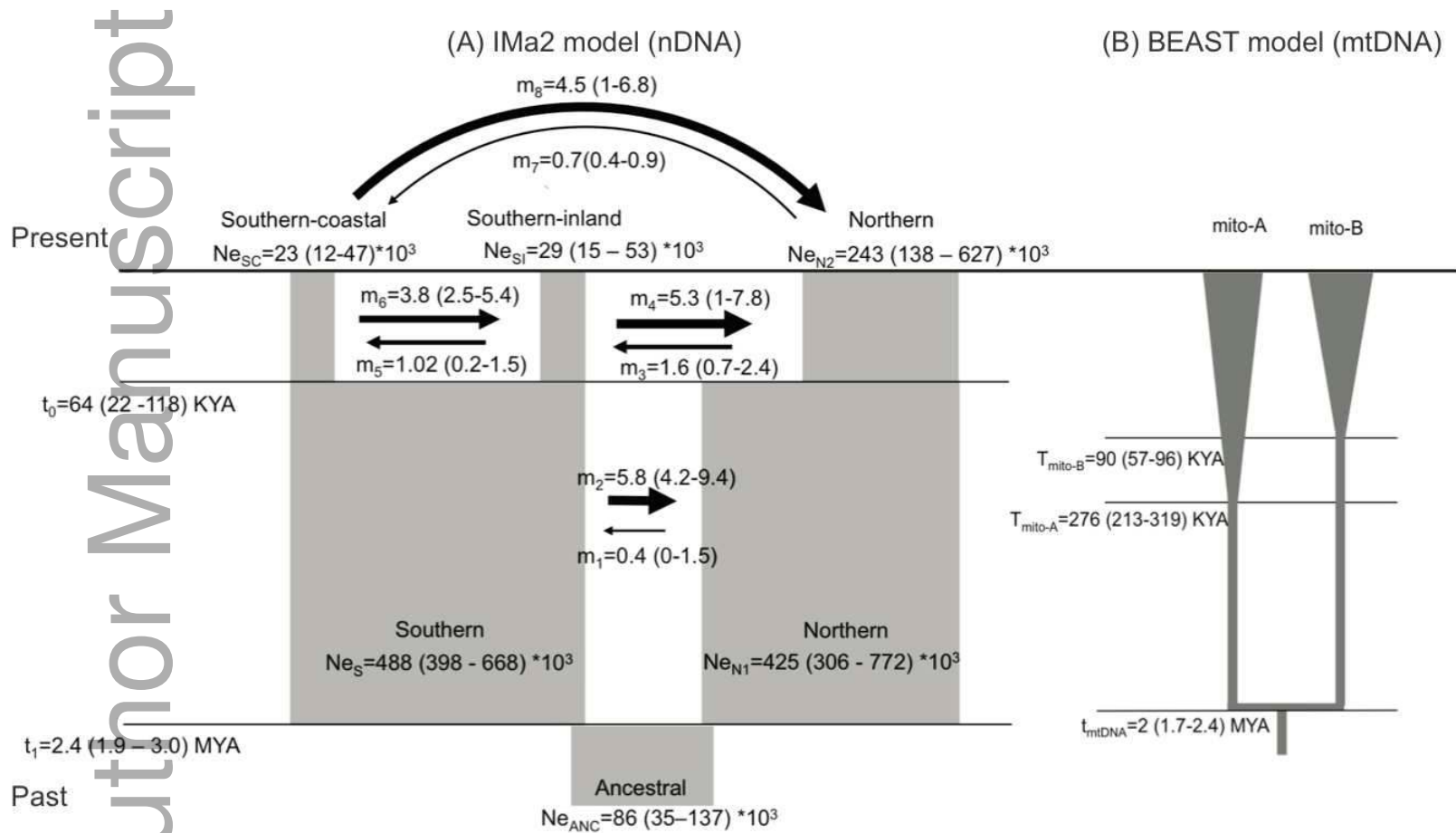


Figure 3 Estimates (high point (95%HPDs)) of coalescent analyses in IMa2 (400 nDNA loci) and BEAST (10 mtDNA genes). (A) IMa2 model. Divergence times: (t_1) northern vs southern ancestral populations; (t_0) southern coastal vs. southern inland populations. Effective population size (Ne): (Ne_{ANC}) ancestral root population; (Ne_{N1}) ancestral northern population; (Ne_S) ancestral southern population; (Ne_{N2}) northern

population; ($N_{e_{SC}}$) southern coastal population; ($N_{e_{SI}}$) southern inland population. Gene flow: ($m1$) ancestral northern to ancestral southern; ($m2$) ancestral southern to ancestral northern; ($m3$) northern to southern inland; ($m4$) southern inland to northern; ($m5$) southern inland to southern coastal; ($m6$) southern coastal to southern inland; ($m7$) northern to southern coastal; ($m8$) southern coastal to northern. (B) BEAST mitolineage model. Divergence times (t_{mtDNA}) between mitolineages mito-A and mito-B. Time to the most recent common ancestor (TMRCA) for ($T_{\text{mito-A}}$) mitolineage mito-A and ($T_{\text{mito-B}}$) mitolineage mito-B indicate probable times of mitochondrial selective sweeps.

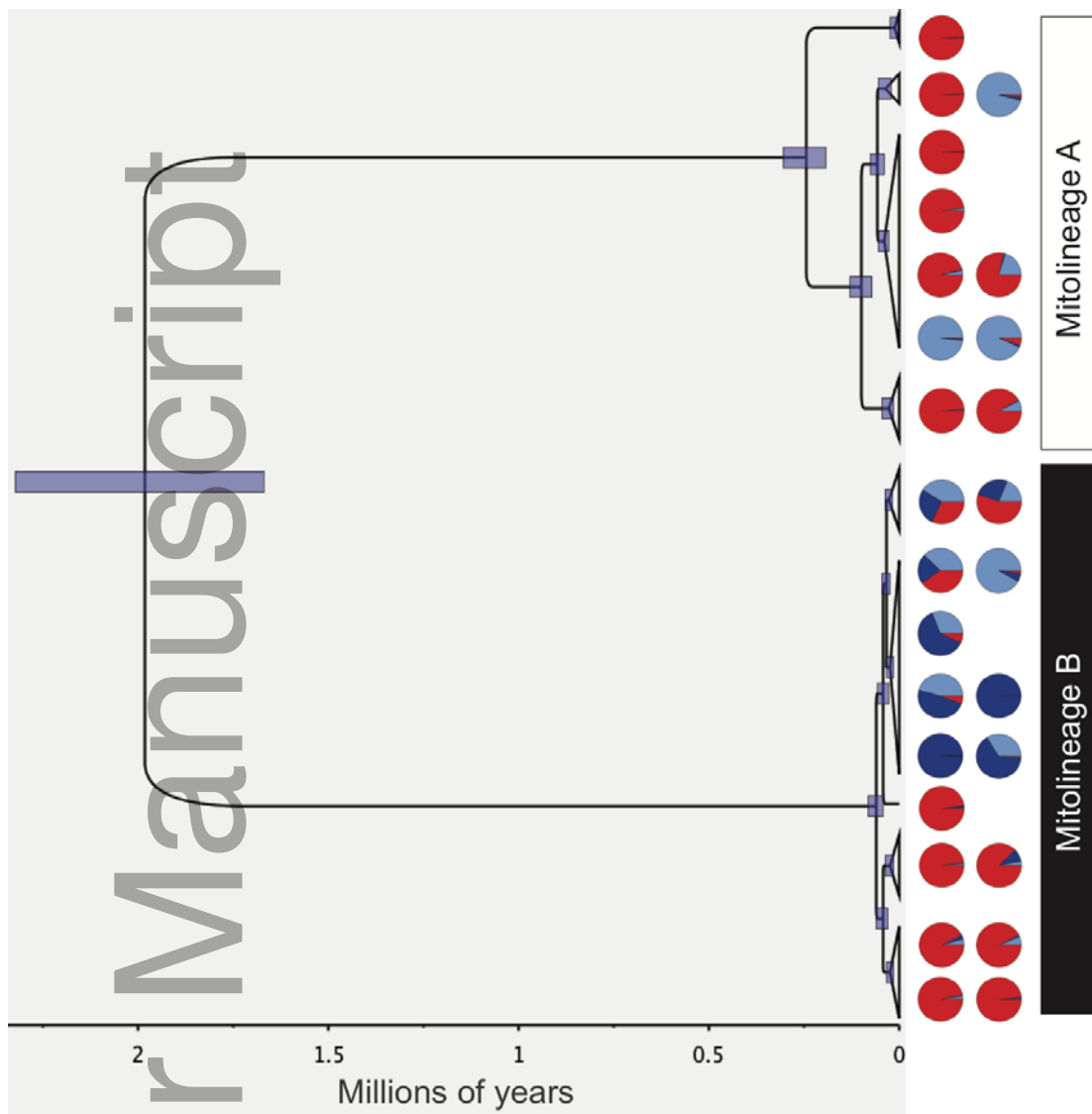


Figure 4 Phylogenetic tree reconstructed by BEAST from 10 mitochondrial genes. The 95% HDP of the time estimates are shown with blue bars in the tree nodes. The two mitolineages are shown with white (mito-A) and black (mito-B) rectangles as in Fig. 1A. The northernmost sample of mito-A mitolineage displays late-Pleistocene intra-lineage divergence. Samples for which nuclear loci were also sequenced are shown with individual pie charts reflecting their population assignment membership as in Fig. 1B: northern population (red), southern coastal population (dark blue) and southern inland population (light blue). All major nodes are fully supported (PP = 1.0). For more details including node support values, expanded terminal tips and individual labels see Fig. S6.

1 REFERENCES

- 2 Amos JN, Harrisson KA, Radford JQ, *et al.* (2014) Species - and sex - specific connectivity effects of
3 habitat fragmentation in a suite of woodland birds. *Ecology* **95**, 1556-1568.
- 4 Antao T, Lopes A, Lopes RJ, Beja-Pereira A, Luikart G (2008) LOSITAN: a workbench to detect
5 molecular adaptation based on a Fst-outlier method. *BMC Bioinformatics* **9**, 323.
- 6 Ballard JWO, Melvin RG (2010) Linking the mitochondrial genotype to the organismal phenotype.
7 *Molecular Ecology* **19**, 1523-1539.
- 8 Bar-Yaacov D, Blumberg A, Mishmar D (2012) Mitochondrial-nuclear co-evolution and its effects on
9 OXPHOS activity and regulation. *Biochimica et Biophysica Acta (BBA)-Gene Regulatory*
10 *Mechanisms* **1819**, 1107-1111.
- 11 Barrows TT, Stone JO, Fifield LK, Cresswell RG (2002) The timing of the last glacial maximum in
12 Australia. *Quaternary science reviews* **21**, 159-173.
- 13 Beck EA, Thompson AC, Sharbrough J, Brud E, Llopart A (2015) Gene flow between *Drosophila*
14 *yakuba* and *Drosophila santomea* in subunit V of cytochrome c oxidase: A potential case of
15 cytonuclear cointrogression. *Evolution* **69**, 1973-1986.
- 16 Boratyński Z, Ketola T, Koskela E, Mappes T (2016) The Sex Specific Genetic Variation of Energetics in
17 Bank Voles, Consequences of Introgression? *Evolutionary Biology* **43**, 37-47.
- 18 Boratyński Z, Melo-Ferreira J, Alves P, *et al.* (2014) Molecular and ecological signs of mitochondrial
19 adaptation: consequences for introgression? *Heredity* **113**, 277-286.
- 20 Boyd R, Roy DP (1995) *Quaternary Geology of the Hunter Valley: Excursion Guide* Department of
21 Geology, The University of Newcastle.
- 22 Bryant LM, Krosch MN (2016) Lines in the land: a review of evidence for eastern Australia's major
23 biogeographical barriers to closed forest taxa. *Biological Journal of the Linnean Society*.
- 24 Burton RS, Pereira RJ, Barreto FS (2013) Cytonuclear Genomic Interactions and Hybrid Breakdown.
25 *Annual Review of Ecology, Evolution, and Systematics* **44**, 281-302.
- 26 Byrne M, Steane DA, Joseph L, *et al.* (2011) Decline of a biome: evolution, contraction,
27 fragmentation, extinction and invasion of the Australian mesic zone biota. *Journal of*
28 *Biogeography* **38**, 1635-1656.
- 29 Byrne M, Yeates D, Joseph L, *et al.* (2008) Birth of a biome: insights into the assembly and
30 maintenance of the Australian arid zone biota. *Molecular Ecology* **17**, 4398-4417.
- 31 Camacho C, Coulouris G, Avagyan V, *et al.* (2009) BLAST+: architecture and applications. *BMC*
32 *Bioinformatics* **10**, 1.

- 33 Camus MF, Wolf JB, Morrow EH, Dowling DK (2015) Single Nucleotides in the mtDNA Sequence
34 Modify Mitochondrial Molecular Function and Are Associated with Sex-Specific Effects on
35 Fertility and Aging. *Current Biology* **25**, 2717-2722.
- 36 Crandall KA, Bininda-Emonds OR, Mace GM, Wayne RK (2000) Considering evolutionary processes in
37 conservation biology. *Trends in Ecology & Evolution* **15**, 290-295.
- 38 Currat M, Ruedi M, Petit RJ, Excoffier L (2008) The hidden side of invasions: massive introgression by
39 local genes. *Evolution* **62**, 1908-1920.
- 40 Das J (2006) The role of mitochondrial respiration in physiological and evolutionary adaptation.
41 *BioEssays* **28**, 890-901.
- 42 Debus S, Ford H (2012) Responses of Eastern Yellow Robins *Eopsaltria australis* to translocation into
43 vegetation remnants in a fragmented landscape. *Pacific Conservation Biology* **18**, 194-202.
- 44 DePristo MA, Banks E, Poplin R, *et al.* (2011) A framework for variation discovery and genotyping
45 using next-generation DNA sequencing data. *Nature genetics* **43**, 491-498.
- 46 Deremiens L, Schwartz L, Angers A, Glémet H, Angers B (2015) Interactions between nuclear genes
47 and a foreign mitochondrial genome in the redbelly dace *Chrosomus eos*. *Comparative*
48 *Biochemistry and Physiology Part B: Biochemistry and Molecular Biology* **189**, 80-86.
- 49 Doiron S, Bernatchez L, Blier PU (2002) A comparative mitogenomic analysis of the potential
50 adaptive value of arctic charr mtDNA introgression in brook charr populations (*Salvelinus*
51 *fontinalis* Mitchill). *Molecular Biology and Evolution* **19**, 1902-1909.
- 52 Dowling DK, Friberg U, Lindell J (2008) Evolutionary implications of non-neutral mitochondrial
53 genetic variation. *Trends in Ecology and Evolution* **23**, 546-554.
- 54 Drummond AJ, Suchard MA, Xie D, Rambaut A (2012) Bayesian phylogenetics with BEAUti and the
55 BEAST 1.7. *Molecular Biology and Evolution* **29**, 1969-1973.
- 56 Earl DA (2012) STRUCTURE HARVESTER: a website and program for visualizing STRUCTURE output
57 and implementing the Evanno method. *Conservation Genetics Resources* **4**, 359-361.
- 58 Ellegren H (2007) Molecular evolutionary genomics of birds. *Cytogenetic and genome research* **117**,
59 120-130.
- 60 Evanno G, Regnaut S, Goudet J (2005) Detecting the number of clusters of individuals using the
61 software STRUCTURE: a simulation study. *Molecular Ecology* **14**, 2611-2620.
- 62 Ford J (1979) Speciation or subspeciation in the yellow robins? *Emu* **79**, 103-106.
- 63 Ford J (1987) Minor isolates and minor geographical barriers in avian speciation in continental
64 Australia. *Emu* **87**, 90-102.

- 65 Funk DJ, Omland KE (2003) Species-level paraphyly and polyphyly: frequency, causes, and
66 consequences, with insights from animal mitochondrial DNA. *Annual Review of Ecology,
67 Evolution, and Systematics*, 397-423.
- 68 Gershoni M, Templeton AR, Mishmar D (2009) Mitochondrial bioenergetics as a major motive force
69 of speciation. *BioEssays* **31**, 642-650.
- 70 Haldane JB (1922) Sex ratio and unisexual sterility in hybrid animals. *Journal of genetics* **12**, 101-109.
- 71 Harrison RG (1990) Hybrid zones: windows on evolutionary process. *Oxford surveys in evolutionary
72 biology* **7**, 69-128.
- 73 Harrison RG, Larson EL (2014) Hybridization, Introgression, and the Nature of Species Boundaries.
74 *Journal of Heredity* **105**, 795-809.
- 75 Harrison RG, Larson EL (2016) Heterogeneous genome divergence, differential introgression, and the
76 origin and structure of hybrid zones. *Molecular Ecology*.
- 77 Harrison KA, Pavlova A, Amos JN, *et al.* (2012) Fine-scale effects of habitat loss and fragmentation
78 despite large-scale gene flow for some regionally declining woodland bird species.
79 *Landscape ecology* **27**, 813-827.
- 80 Hedrick PW (2013) Adaptive introgression in animals: examples and comparison to new mutation
81 and standing variation as sources of adaptive variation. *Molecular Ecology* **22**, 4606-4618.
- 82 Hey J (2010) Isolation with Migration Models for More Than Two Populations. *Molecular Biology and
83 Evolution* **27**, 905-920.
- 84 Hey J, Nielsen R (2004) Multilocus methods for estimating population sizes, migration rates and
85 divergence time, with applications to the divergence of *Drosophila pseudoobscura* and *D.*
86 *persimilis*. *Genetics* **167**, 747-760.
- 87 Higgins P, Peter J (2002) Volume 6: Pardalotes to Shrike-thrushes. Handbook of Australian, New
88 Zealand and Antarctic Birds. Melbourne: Oxford University Press.
- 89 Hill GE (2015) Mitonuclear ecology. *Molecular Biology and Evolution* **32**, 1917-1927.
- 90 Hill GE (2016) Mitonuclear coevolution as the genesis of speciation and the mitochondrial DNA
91 barcode gap. *Ecology and evolution* **22**, 5831-5842.
- 92 Hill GE, Johnson JD (2013) The mitonuclear compatibility hypothesis of sexual selection. *Proceedings
93 of the Royal Society of London B: Biological Sciences* **280**, 20131314.
- 94 Hocknull SA, Zhao J-x, Feng Y-x, Webb GE (2007) Responses of Quaternary rainforest vertebrates to
95 climate change in Australia. *Earth and Planetary Science Letters* **264**, 317-331.
- 96 Jakobsson M, Rosenberg NA (2007) CLUMPP: a cluster matching and permutation program for
97 dealing with label switching and multimodality in analysis of population structure.
98 *Bioinformatics* **23**, 1801-1806.

- 99 Jombart T, Ahmed I (2011) adegenet 1.3-1: new tools for the analysis of genome-wide SNP data.
100 *Bioinformatics* **27**, 3070-3071.
- 101 Jombart T, Devillard S, Balloux F (2010) Discriminant analysis of principal components: a new
102 method for the analysis of genetically structured populations. *BMC genetics* **11**, 94.
- 103 Joseph L, Omland KE (2009) Phylogeography: its development and impact in Australo-Papuan
104 ornithology with special reference to paraphyly in Australian birds. *Emu* **109**, 1-23.
- 105 Kearns AM, Joseph L, Toon A, Cook LG (2014) Australia's arid-adapted butcherbirds experienced
106 range expansions during Pleistocene glacial maxima. *Nature communications* **5**, article
107 n°3994.
- 108 Kimura M, Maruyama T, Crow JF (1963) The mutation load in small populations. *Genetics* **48**, 1303.
- 109 Lanfear R, Calcott B, Ho SY, Guindon S (2012) PartitionFinder: combined selection of partitioning
110 schemes and substitution models for phylogenetic analyses. *Molecular Biology and Evolution*
111 **29**, 1695-1701.
- 112 Lee JY, Edwards SV (2008) Divergence Across Australia's Carpentarian Barrier: Statistical
113 Phylogeography of the Red-Backed Fairy Wren (*Malurus melanocephalus*). *Evolution* **62**,
114 3117-3134.
- 115 Lemmon AR, Emme SA, Lemmon EM (2012) Anchored hybrid enrichment for massively high-
116 throughput phylogenomics. *Systematic biology* **61**, 721-744.
- 117 Lerner HR, Meyer M, James HF, Hofreiter M, Fleischer RC (2011) Multilocus resolution of phylogeny
118 and timescale in the extant adaptive radiation of Hawaiian honeycreepers. *Current Biology*
119 **21**, 1838-1844.
- 120 Levin L, Blumberg A, Barshad G, Mishmar D (2014) Mito-nuclear co-evolution: the positive and
121 negative sides of functional ancient mutations. *Frontiers in Genetics* **5**, 448.
- 122 Li H, Durbin R (2009) Fast and accurate short read alignment with Burrows–Wheeler transform.
123 *Bioinformatics* **25**, 1754-1760.
- 124 Li R, Zhu H, Ruan J, *et al.* (2010) De novo assembly of human genomes with massively parallel short
125 read sequencing. *Genome Research* **20**, 265-272.
- 126 Llopart A, Herrig D, Brud E, Stecklein Z (2014) Sequential adaptive introgression of the mitochondrial
127 genome in *Drosophila yakuba* and *Drosophila santomea*. *Molecular Ecology* **23**, 1124-1136.
- 128 Mallet J (2005) Hybridization as an invasion of the genome. *Trends in Ecology & Evolution* **20**, 229-
129 237.
- 130 McFarlane SE, Sirkiä PM, Ålund M, Qvarnström A (2016) Hybrid Dysfunction Expressed as Elevated
131 Metabolic Rate in Male Ficedula Flycatchers. *PLoS One* **11**, e0161547.

- 132 Morales HE, Pavlova A, Joseph L, Sunnucks P (2015) Positive and purifying selection in mitochondrial
133 genomes of a bird with mitonuclear discordance. *Molecular Ecology* **24**, 2820–2837.
- 134 Morales HE, Pavlova A, Sunnucks P, *et al.* (2016a) Neutral and selective drivers of colour evolution in
135 a widespread Australian passerine. *Journal of Biogeography* (*in press*).
- 136 Morales HE, Pavlova A, Amos N, *et al.* (2016b) Mitochondrial-nuclear interactions maintain a deep
137 mitochondrial split in the face of nuclear gene flow. *bioRxiv*.
- 138 Narum SR (2006) Beyond Bonferroni: less conservative analyses for conservation genetics.
139 *Conservation Genetics* **7**, 783-787.
- 140 Nei M (1973) Analysis of gene diversity in subdivided populations. *Proceedings of the National*
141 *Academy of Sciences* **70**, 3321-3323.
- 142 Ohta T (2002) Near-neutrality in evolution of genes and gene regulation. *Proceedings of the National*
143 *Academy of Sciences* **99**, 16134-16137.
- 144 Pavlova A, Amos JN, Joseph L, *et al.* (2013) Perched at the mito - nuclear crossroads: divergent
145 mitochondrial lineages correlate with environment in the face of ongoing nuclear gene flow
146 in an Australian bird. *Evolution* **67**, 3412-3428.
- 147 Payseur BA (2010) Using differential introgression in hybrid zones to identify genomic regions
148 involved in speciation. *Molecular ecology resources* **10**, 806-820.
- 149 Percival I, Meakin N, Sherwin L, Vanderlaan T, Flitcroft P (2012) Permian fossils and
150 palaeoenvironments of the northern Sydney Basin. *New South Wales. Geological Survey of*
151 *NSW Quarterly Notes* **138**, 1-23.
- 152 Pereira RJ, Barreto FS, Burton RS (2014) Ecological novelty by hybridization: experimental evidence
153 for increased thermal tolerance by transgressive segregation in *Tigriopus californicus*.
154 *Evolution* **68**, 204-215.
- 155 Petit RJ, Bodénès C, Ducouso A, Roussel G, Kremer A (2004) Hybridization as a mechanism of
156 invasion in oaks. *New Phytologist* **161**, 151-164.
- 157 Petit RJ, Excoffier L (2009) Gene flow and species delimitation. *Trends in Ecology and Evolution* **24**,
158 386-393.
- 159 Porch N (2010) Climate space, bioclimatic envelopes and coexistence methods for the reconstruction
160 of past climates: a method using Australian beetles and significance for Quaternary
161 reconstruction. *Quaternary science reviews* **29**, 633-647.
- 162 Pritchard JK, Stephens M, Donnelly P (2000) Inference of population structure using multilocus
163 genotype data. *Genetics* **155**, 945-959.
- 164 Prum RO, Berv JS, Dornburg A, *et al.* (2015) A comprehensive phylogeny of birds (Aves) using
165 targeted next-generation DNA sequencing. *Nature* **526**, 569-573.

- 166 Pyron RA, Hsieh FW, Lemmon AR, Lemmon EM, Hendry CR (2016) Integrating phylogenomic and
167 morphological data to assess candidate species - delimitation models in brown and red -
168 bellied snakes (*Storeria*). *Zoological Journal of the Linnean Society* **177**, 937–949.
- 169 R Development Core Team (2014) R: A language and environment for statistical computing. R
170 Foundation for Statistical Computing, Vienna, Austria. ISBN 3-900051-07-0.
- 171 Rambaut A, Pybus OG, Nelson MI, *et al.* (2008) The genomic and epidemiological dynamics of human
172 influenza A virus. *Nature* **453**, 615-619.
- 173 Rambaut A, Suchard M, Xie D, Drummond A (2014) Tracer v1. 6, Available from
174 <http://beast.bio.ed.ac.uk/Tracer>.
- 175 Rheindt FE, Edwards SV (2011) Genetic introgression: an integral but neglected component of
176 speciation in birds. *The Auk* **128**, 620-632.
- 177 Rieseberg LH (2009) Evolution: replacing genes and traits through hybridization. *Current Biology* **19**,
178 R119-R122.
- 179 Roca AL, Georgiadis N, O'Brien SJ (2005) Cytonuclear genomic dissociation in African elephant
180 species. *Nature genetics* **37**, 96-100.
- 181 Saltré F, Rodríguez-Rey M, Brook BW, *et al.* (2016) Climate change not to blame for late Quaternary
182 megafauna extinctions in Australia. *Nature communications* **29**, 10511.
- 183 Schodde R (2006) Australia's bird fauna today—origins and evolutionary development. *Evolution and*
184 *Biogeography of Australasian Vertebrates. Auscipub, Oatlands, New South Wales*, 413-458.
- 185 Schodde R, Mason I (1999) *Directory of Australian Birds: Passerines: Passerines* CSIRO PUBLISHING.
- 186 Seehausen O, Butlin RK, Keller I, *et al.* (2014) Genomics and the origin of species. *Nature Review*
187 *Genetics* **15**, 176-192.
- 188 Shaw KL, Mullen SP (2014) Speciation continuum. *Journal of Heredity* **105**, 741-742.
- 189 Shipham A, Schmidt DJ, Joseph L, Hughes JM (2015) Phylogenetic analysis of the Australian rosella
190 parrots (*Platycercus*) reveals discordance among molecules and plumage. *Molecular*
191 *phylogenetics and evolution* **91**, 150-159.
- 192 Shipham A, Schmidt DJ, Joseph L, Hughes JM (2016) A genomic approach reinforces a hypothesis of
193 mitochondrial capture in eastern Australian rosellas. *The Auk* **134**, 181-192.
- 194 Sloan DB, Havird JC, Sharbrough J (2016) The On - Again, Off - Again Relationship between
195 Mitochondrial Genomes and Species Boundaries. *Molecular Ecology*.
- 196 Sniderman J (2011) Early Pleistocene vegetation change in upland south - eastern Australia. *Journal*
197 *of Biogeography* **38**, 1456-1470.

- 198 Sniderman J, Porch N, Kershaw AP (2009) Quantitative reconstruction of Early Pleistocene climate in
199 southeastern Australia and implications for atmospheric circulation. *Quaternary science*
200 *reviews* **28**, 3185-3196.
- 201 Thomson R, Pritchard JK, Shen P, Oefner PJ, Feldman MW (2000) Recent common ancestry of human
202 Y chromosomes: evidence from DNA sequence data. *Proceedings of the National Academy of*
203 *Sciences* **97**, 7360-7365.
- 204 Toews DP, Brelsford A (2012) The biogeography of mitochondrial and nuclear discordance in animals.
205 *Molecular Ecology* **21**, 3907-3930.
- 206 Wallace DC (2005) A mitochondrial paradigm of metabolic and degenerative diseases, aging, and
207 cancer: a dawn for evolutionary medicine. *Annual review of genetics* **39**, 359.
- 208 Warren WC, Clayton DF, Ellegren H, *et al.* (2010) The genome of a songbird. *Nature* **464**, 757-762.
- 209 Winter DJ (2012) MMOD: an R library for the calculation of population differentiation statistics.
210 *Molecular ecology resources* **12**, 1158-1160.
- 211 Woerner AE, Cox MP, Hammer MF (2007) Recombination-filtered genomic datasets by information
212 maximization. *Bioinformatics* **23**, 1851-1853.
- 213 Wolff JN, Pichaud N, Camus MF, *et al.* (2016) Evolutionary implications of mitochondrial genetic
214 variation: mitochondrial genetic effects on OXPHOS respiration and mitochondrial quantity
215 change with age and sex in fruit flies. *Journal of evolutionary biology* **29**, 736-747.

216

217 **Author Contributions**

218 HM, AP and PS designed the research. LJ provided museum samples. HM produced and
219 analysed the data. All the authors contributed to the concepts and paper writing.

220

221 **Supporting Information:**

222 Table S1 Samples screened for nuclear DNA (nDNA) and mitochondrial ND2 variation

223 Table S2 Samples screened for mitochondrial genome

224 Table S3 Partitions for the BEAST analysis and substitution models according to
225 PartitionFinder

226 Table S4 Parameter estimates for coalescent analyses in BEAST and IMa2

227 Figure S1 Convergence plots for STRUCTURE K = 2

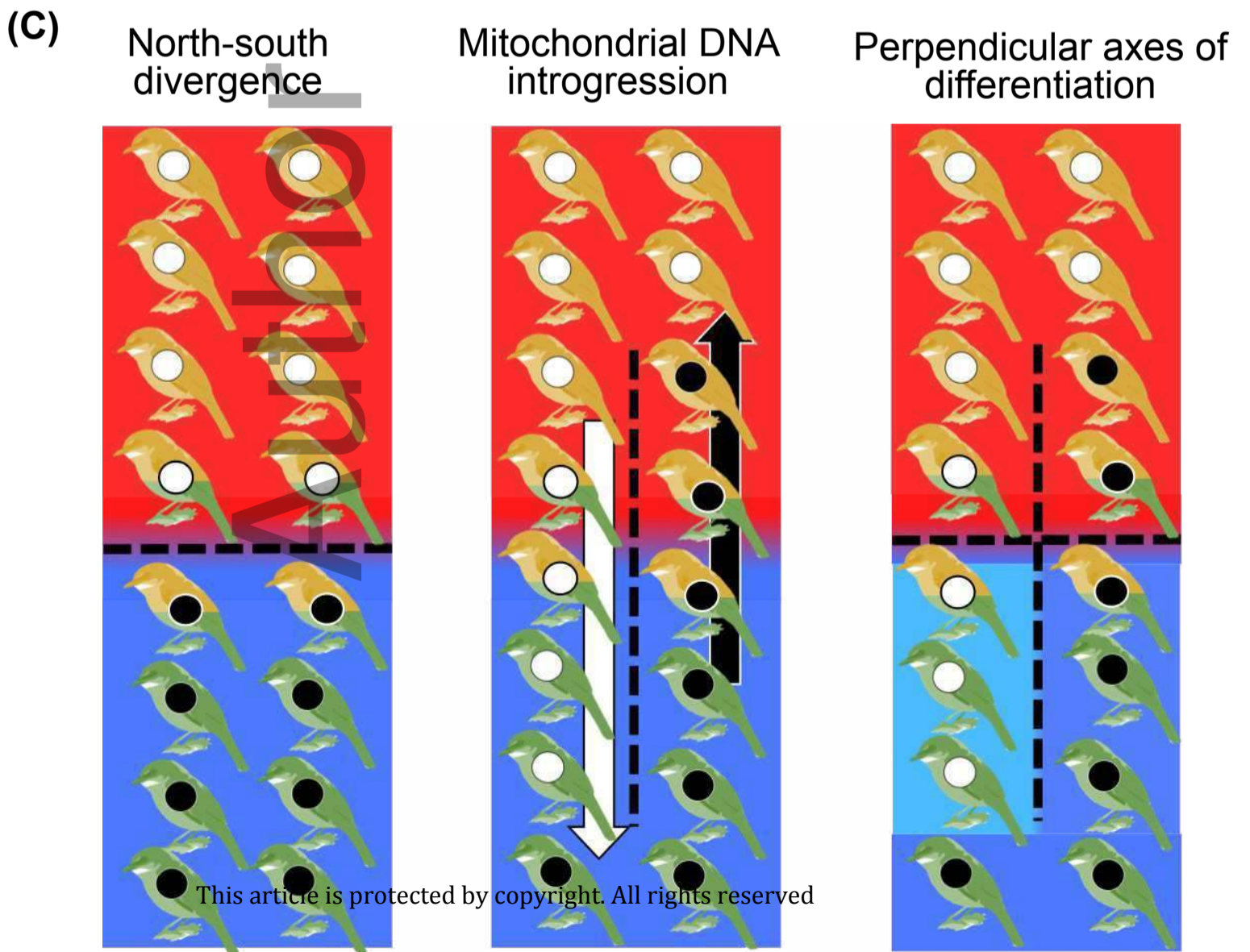
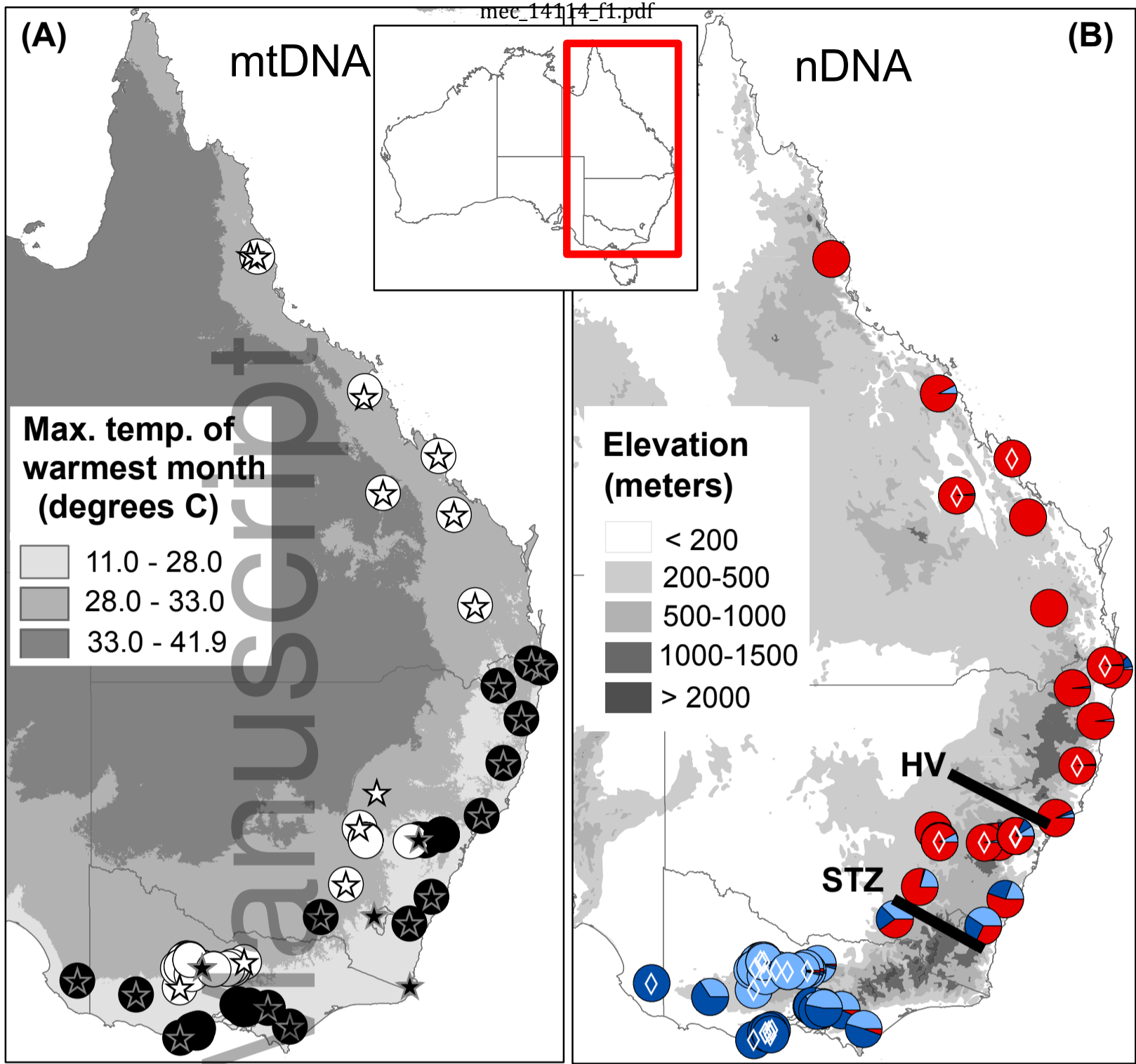
228 Figure S2 Convergence plots for STRUCTURE K = 3

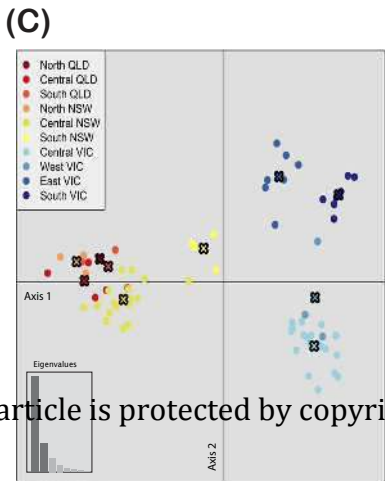
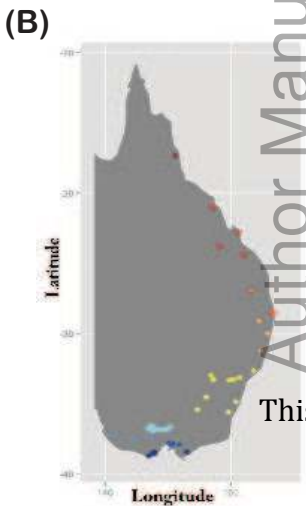
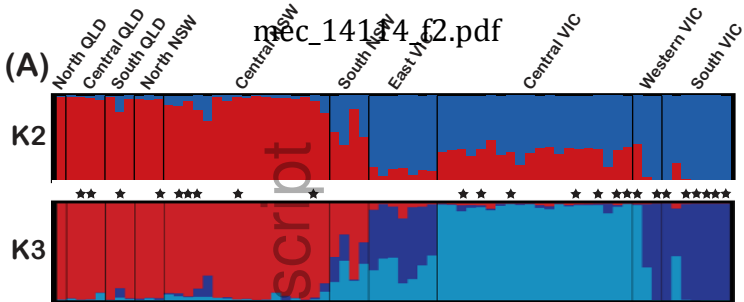
229 Figure S3 Delta likelihood for STRUCTURE analysis with populations K = 1-5

230 Figure S4 G_{ST} differentiation between STRUCTURE K = 3 populations

- 231 Figure S5 Posterior distributions for IMA2 model
- 232 Figure S6 Phylogenetic tree reconstructed by BEAST from 10 mitochondrial genes
- 233
- 234 **Data access in <https://doi.org/10.6084/m9.figshare.3581004.v2>:**
- 235 Sample Information
- 236 Hybrid capture probes design
- 237 BLAST output file
- 238 Fasta alignment files of nDNA loci
- 239 SNP data
- 240 Alignment of 10 mtDNA genes in nexus format

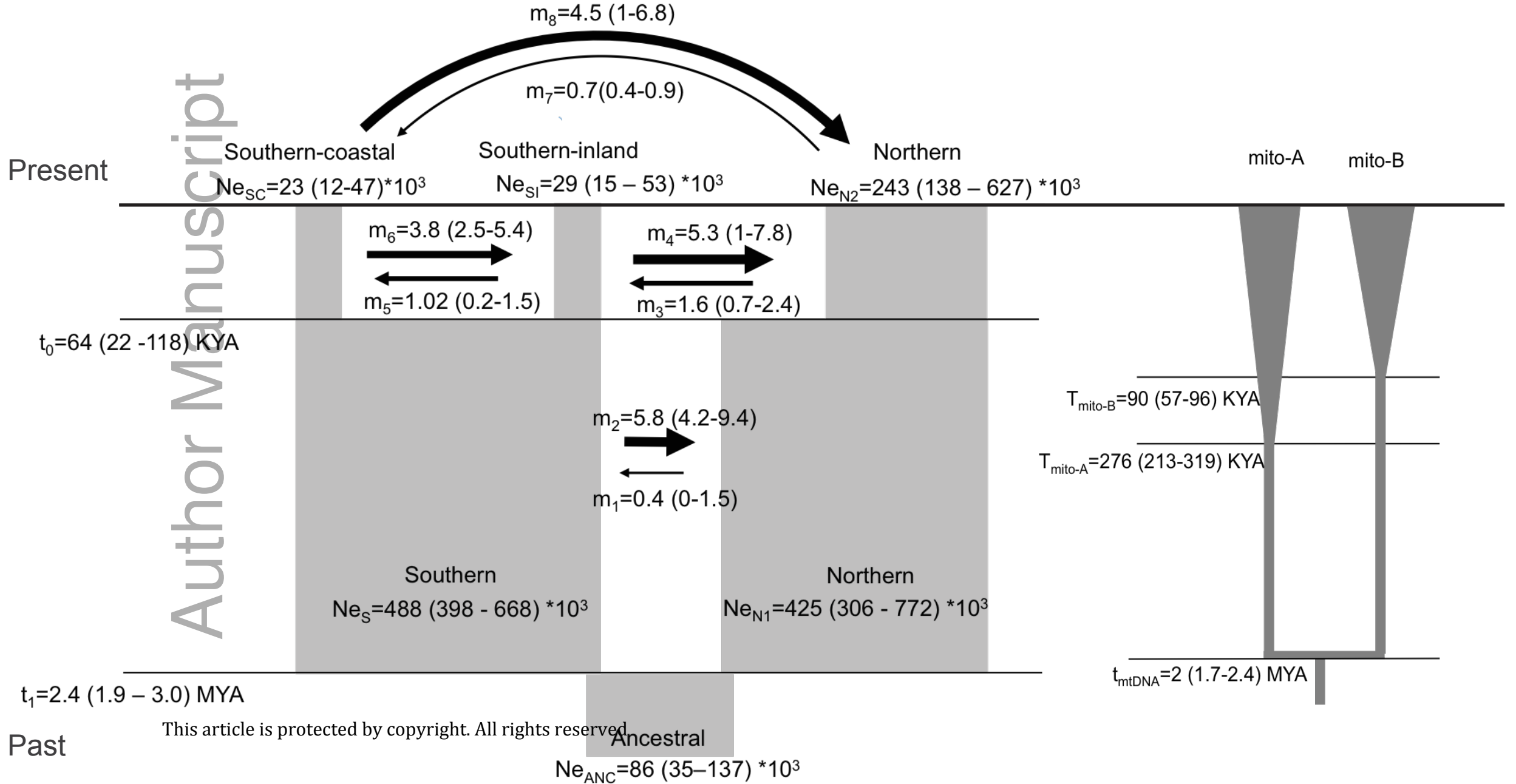
Author Manuscript





(A) IMA2 model (nDNA)

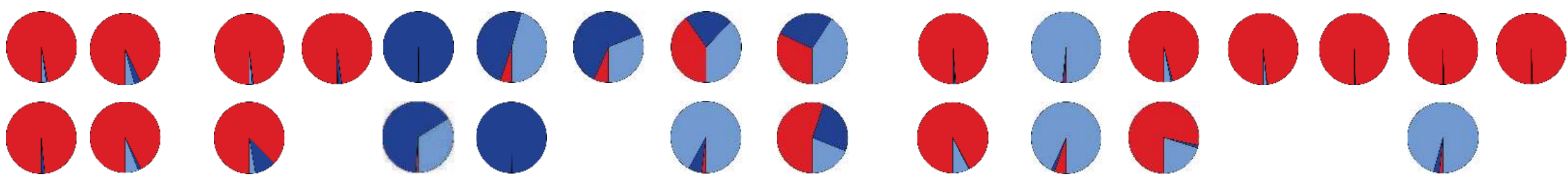
(B) BEAST model (mtDNA)



2
1.5
1
0.5
0
Millions of years

Author Manuscript

This article is protected by copyright. All rights reserved



Mitolineage B

Mitolineage A

